Atmospheric Research 102 (2011) 452–459

Contents lists available at SciVerse ScienceDirect

Atmospheric Research

journal homepage: www.elsevier.com/locate/atmos

Effects of cirrus cloudiness on solar irradiance in four spectral bands

A. Kazantzidis [a,*], K. Eleftheratos [b,c], C.S. Zerefos [b,c]

[a] Laboratory of Atmospheric Physics, Department of Physics, University of Patras, Greece
[b] Laboratory of Climatology & Atmospheric Environment, Faculty of Geology & Geoenvironment, N.K.U.A., Greece
[c] Biomedical Research Foundation, Academy of Athens, Greece

ARTICLE INFO

Article history:
Received 3 April 2011
Received in revised form 28 September 2011
Accepted 28 September 2011

Keywords:
Cirrus clouds
Cloud optical properties
Solar radiation
Ultraviolet radiation
Photosynthetically active radiation
Radiative transfer

ABSTRACT

The impact of cirrus cloudiness on solar irradiance is estimated with the use of a cloud climatology (coverage, optical thickness) and a radiative transfer model. The change in irradiance in four spectral bands (shortwave, photosynthetically active radiation and ultraviolet A and B integrals) due to cirrus clouds at different height levels between the cloud base and the ground is examined for different solar zenith angles. The disproportionate role of the cirrus cloud layer, due to the different contribution of the direct and the diffuse irradiance components, is revealed. The average effect of cirrus clouds on solar irradiance is, in many cases, comparable with the measuring uncertainties of remote sensing instruments. This result indicates that, the detection of cirrus clouds and the determination or parameterization of their optical properties will significantly reduce the uncertainty of tropospheric measurements of several atmospheric constituents.

1. Introduction

Cirrus clouds are the most common type of high-level clouds forming in the vicinity of the tropopause. They are optically thin, non-black, high, cold clouds composed of ice crystals. Along with low marine stratus clouds, they are the principal cloud type controlling the Earth's radiation budget (Lynch, 1996). Thin cirrus clouds are of significant climatological importance, because they produce net heating of the planet. Their relatively large particles scatter sunlight efficiently into the forward (downward) direction and, thus, they do not prevent sunlight from reaching the Earth. In the thermal infrared, ice is highly absorptive (and thus highly emissive) and it reradiates part of the energy it receives from the Earth back to the planet (Liou, 1986).

The radiative effects of natural and manmade cirrus clouds have been studied extensively in recent years with the use of various datasets, model calculations and parameterizations (e.g. Ramanathan et al., 1989; Meerkötter et al., 1999; Edwards et al., 2007; Lee et al., 2009; Min et al., 2010; Burkhardt et al., 2010). Those studies revealed the significant influence of cirrus clouds in the propagation of solar and infrared radiation in the atmosphere, but indicated also the limitations of the available observing techniques. As a result, the parameterization of cirrus radiative properties for use in global or regional models is accompanied by relative high uncertainties (Liou, 2005).

Although cirrus clouds are expected to affect quite significantly the radiative forcing at the tropopause, their impact on the vertical distribution of spectral radiation in the troposphere has been slightly examined. Wendisch et al. (2001) and Pilewskie et al. (2003) tried to estimate the effect of clouds over the solar wavelength range, despite the inevitable measurement uncertainties like the need for accurate time synchronization of measurements for heterogeneous clouds. Schmidt et al. (2007) compared cirrus cloud retrievals from satellite and airborne instruments with the use of a three dimensional radiative transfer model and suggested the need for more systematic spectral irradiance and radiance measurements. In a more recent study (Schmidt et al., 2010), the spectral shape of measured apparent absorption in heterogeneous ice clouds was examined.

* Corresponding author.
E-mail address: akaza@upatras.gr (A. Kazantzidis).

0169-8095/$ – see front matter © 2011 Elsevier B.V. All rights reserved.
doi:10.1016/j.atmosres.2011.09.015

In the present study, we use 24 years of data from the International Satellite Cloud Climatology Project (ISCCP) and analyze the impact on solar irradiance from the existence of cirrus clouds. To avoid difficulties and uncertainties that are introduced in measurements and model calculations, we use a spectral radiative transfer model to calculate the percentage changes of irradiance in four spectral bands (from ultraviolet to shortwave) due to cirrus clouds. The goal is to investigate, for the first time, the changes in solar irradiance at different heights in the troposphere induced by natural and manmade cirrus clouds and underline the importance of accurate detection methods and parameterizations to reduce the uncertainties of remote sensing measurements and model calculations.

2. Cirrus cloud data

The cloud dataset analyzed in this study is produced by the International Satellite Cloud Climatology Project (ISCCP) (Rossow and Schiffer, 1991, 1999). The data are based on observations from a suite of operational geostationary and polar orbiting satellites and contain detailed information about the distribution of cloud radiative properties and their diurnal and seasonal variations. Visible (VIS) radiances are used to retrieve the optical thickness of clouds and infrared (IR) radiances to retrieve cloud top temperature and pressure. The D2 dataset, used in this study, has a spatial resolution of 280 km (~2.5° at the equator) and provides monthly averages of cloud properties from fifteen different cloud types. The derived cloud types are based on radiometric definitions that rely on cloud optical thickness and cloud top pressure. Cirrus clouds are defined as those with optical thickness less than 3.6 and cloud top pressure less than 440 hPa. In this study, we use the cirrus cloud data for two months (January and July) during the 1984–2007 time period and examine the effect on irradiance. ISCCP cirrus cloud data have been widely used in several studies (e.g., Stordal et al., 2005; Eleftheratos et al., 2007; Zerefos et al., 2007). High clouds from ISCCP have been compared extensively (Rossow and Schiffer, 1999) against satellite datasets from the Stratospheric Aerosol Gas Experiments (SAGE, Liao et al., 1995) and the High-Resolution Infrared Sounder (HIRS, Jin et al., 1996; Stubenrauch et al., 1999). According to those studies, the total VIS/IR high cloud optical depth is underestimated by 0.05–0.1 in the ISCCP.

Eight regions have been intentionally selected in order to include the effect of both natural and contrail cirrus on solar irradiance. By examining the fuel emissions at cruising altitude (about 9–10 km), we determined adjacent regions over the Northern Hemisphere, which correspond to different air traffic load. The selected regions correspond to the USA, Europe, North Atlantic and North Pacific high and low air traffic corridors and are shown in Fig. 1. The air traffic density was examined by analyzing the aviation fuel consumption inventory in the year 2000 from the Integrated Project QUANTIFY (http://ip-quantify.eu).

It would be expected that persistent contrails would increase cirrus cloud cover over regions with high traffic, when compared to areas with lower air traffic. This has been already examined in previous studies (Zerefos et al., 2003; Stordal et al., 2005). For the selected regions of this study, the average values of cirrus cloud cover and optical depth for January and July, are presented in Fig. 2. Higher values of cloud cover are revealed over the regions with high traffic only in July. In January, however, they are less, when compared with the values over the low air traffic regions. Similar values of cirrus optical depth are revealed, over high and low air traffic regions, during January. In contrast, increased values of optical depth are shown during July over the high air traffic regions. This result could be a consequence of different cloud climatology in different regions of the Earth. It is out of the scope of this study to examine the reasons of the above mentioned differences, since there are many other factors that contribute to changes in cirrus clouds.

3. Model calculations

In this study, the LibRadtran v1.4 software package (www.libradtran.org, Mayer and Kylling, 2005), was used. LibRadtran

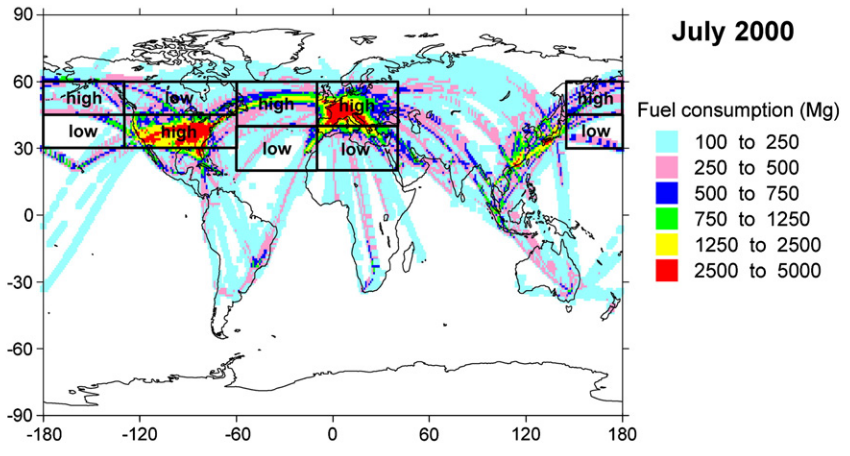

Fig. 1. Aviation fuel consumption (Mg) at about 9–10 km height for the month of July (source: QUANTIFY 2000 emissions inventory). Rectangles correspond to regions with high and low air traffic in which the impact of cirrus clouds have been studied. USA: high air traffic region (30°N–45°N, 60°W–130°W), adjacent low air traffic region (45°N–60°N, 60°W–130°W). Europe: high air traffic region (40°N–60°N, 10°W–40°E), adjacent low air traffic region (20°N–40°N, 10°W–40°E). North Atlantic: high air traffic region (40°N–60°N, 10°W–60°W), adjacent low air traffic region (20°N–40°N, 10°W–60°W). North Pacific: high air traffic region (45°N–60°N, 145°E–130°W), adjacent low air traffic region (30°N–45°N, 145°E–130°W).

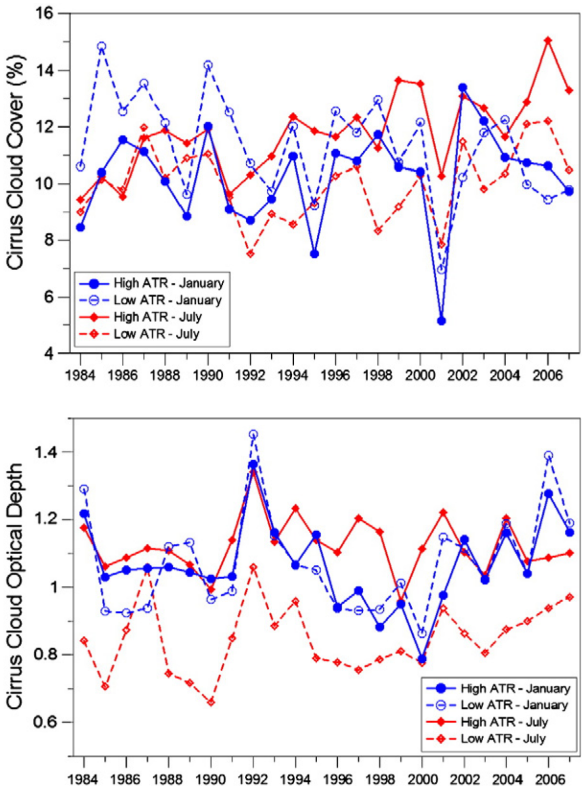

Fig. 2. Time series of average cirrus percentage (%) coverage (upper panel) and optical depth (lower panel) in January and July over the selected high and low air traffic regions (ATR).

has been successfully validated in several model intercomparisons (e.g. van Weele et al., 2000; Cahalan et al., 2005), compared with ground-based measurements (e.g. Bernhard et al., 1998, 2006; Blumthaler et al., 2008), used in synergy with airborne measurements (e.g. Webb et al., 2004; Wendisch et al., 2004; Ehrlich et al., 2009) and satellite estimations (e.g. Borde and Verdebout, 2003; Meerkötter and Bugliaro, 2009; Loyola et al., 2010). The model has also been used for the derivation of aerosol (Kylling et al., 1998; Bais et al., 2005; Meloni et al., 2006) and cloud properties (e.g. Kazantzidis et al., 2001; Cerdena et al., 2007; Kokhanovsky et al., 2007). Based on LibRadtran, the Contrail Cirrus Prediction Tool (CoCiP) has been developed to simulate contrail cirrus, regionally or globally, based on Meteosat data (Schumann, 2010; Schumann et al., 2009).

For the present study, the radiative transfer equation was solved with the DISORT 2.0 algorithm running with 16 streams. The solar irradiance between 290 and 3000 nm with 1 nm step and resolution, based on the extraterrestrial spectrum of Kurucz (1992), was calculated at 1 km step heights, between the ground and the 12 km. The winter and summer Air Force Geophysical Laboratory (AFGL) standard atmospheric vertical profiles of pressure, temperature, ozone, water vapor and other trace gasses over midlatitudes were respectively used for January and July (Anderson et al., 1986). For each region, climatological values of spectral optical properties, derived from the AeroCom project (Kinne et al., 2006), and the vertical profile of Shettle (1989) were accounted for aerosols.

The model runs were performed with and without a layer of cirrus clouds. In both cases, the spectral irradiance calculations were performed at the same height steps and with the same set of input parameters. Since the cloud coverage cannot be inserted in 1-D model calculations, the irradiance derived from the following parameterization:

$$I(\lambda) = N * I_{CL}(\lambda) + (1-N) * I_{CF}(\lambda)$$

where:

- $I(\lambda)$: the spectral irradiance, needed for this study, at wavelength λ
- N: the cloud coverage
- $I_{CL}(\lambda) =$ the spectral irradiance under cloudy (overcast) conditions
- $I_{CF}(\lambda) =$ the spectral irradiance under cloud-free conditions.

The modeled spectra were integrated over four spectral regions, ultraviolet A and B (UVA and UVB), photosynthetically active radiation (PAR) and shortwave (SW), and the percentage (%) differences between cloudy and cloud-free conditions were calculated. The use of percentage differences was selected instead of absolute values, since close to the ground the latter are affected by the use of different values for aerosol optical properties and surface albedo at each region.

The average cirrus cloud cover and optical depth values used in this study are presented in Table 1. The non-linear effect of cloud optical depth on the extinction of solar irradiance was taken into account by using the ISCCP cloud data for each month, year and region as input to the radiative transfer calculations. Then, the average irradiance values during the selected time-period and the percentage differences between cloudy and cloud-free scenarios were calculated. The Fu (1996) parameterization was used for the estimation of the cloud optical properties over the 290–3000 nm spectral region. The cloud layer was placed between 9 and 10 km.

In the above mentioned parameterizations, the differences between contrail and natural cirrus clouds were not taken into account. These differences mainly include the spatial geometry, the effective ice particle sizes and shapes and they are also responsible for different 3-D radiative transfer effects. The separation between natural and anthropogenic ice clouds still remains a large source of uncertainty and additional studies about the spectral properties of contrails, derived from ground-based measurements or satellite images, have been suggested (Yang et al., 2010). Additionally, the 3-D radiative transfer codes have been recently used only in the frame of specific experimental campaigns, providing advanced microphysical and radiative properties of ice clouds, and validated against detailed radiation measurements (O'Hirok and Gautier, 2003; Schmidt et al., 2007, 2010).

4. Results

The percentage (%) difference of irradiance under cloudy and cloud-free conditions was calculated, in order to examine the effect of cloudiness in four spectral bands (UVB, UVA, PAR, SW). It was derived from individual radiative transfer runs for January and July, based on cloud properties

Table 1
Average percentage coverage and optical depth of cirrus clouds for the period 1984–2007 in January and July over selected high and low air traffic regions (ATR) used as input to the radiative transfer calculations.

	January				July			
	Cirrus cover (%)		Optical depth		Cirrus cover (%)		Optical depth	
Region	High ATR	Low ATR	High ATR	Low ATR	High ATR	Low ATR	High ATR	Low ATR
USA	15.9	16.5	0.99	0.96	20.5	18.6	0.80	0.79
Europe	7.2	7.4	1.02	1.04	11.0	6.0	0.81	0.63
N. Atlantic	10.5	12.1	0.98	0.77	9.6	8.1	1.09	0.57
N. Pacific	7.8	10.2	1.17	1.38	5.5	6.9	1.76	1.30

(coverage, optical depth) and averaged over the whole time period (1984–2007) for the selected regions. All results are presented for three solar zenith angles (40°, 60°, 80°) for January and four angles for July (20°, 40°, 60°, 80°).

The calculated differences are summarized at two levels, the ground and the cloud base. The minimum and maximum percentage (%) decreases of UVB, UVA, SW irradiance and PAR, derived from model calculations over all selected regions, due to cirrus cloudiness at these two levels, are presented in Table 2.

In UVB, similar differences are calculated for both months and same solar zenith angles. At the cloud base, they range between 0.5 and 2.2% in January and between 0.3 and 2.4% in July, while the differences are minimum (below 0.5%) for 20° in July. At the ground, all differences between the cloud-free and the cloudy skies are less than 1.6%. In UVA, the greatest differences are revealed also at the cloud base and reach almost 1% for 20° and 40° and 2% for 60°. At 80°, the differences range between 1.3 and 4.5%. The UVA differences are similar in magnitude for 20° and 40° when compared with the results for the UVB region. However, they become higher for 60° and almost double for 80°, revealing the effect of increased percentage of the direct component in UVA irradiance above the cirrus clouds. In this case, more UVA photons penetrate longer optical paths inside the cloud and are scattered away. The UVB direct irradiance is also strongly attenuated inside the cloud, but the diffuse part, which is dominant, is less affected. Most of the difference between the irradiances in the two UV bands at the cloud base is covered in the lower troposphere, due to the increased absorption and scattering of the UVB photons. As a result, their percentage difference at the ground, due to cirrus clouds, is less than 0.3%.

The above described effect in more pronounced in PAR. For both months and lower solar zenith angles, the calculated differences are similar in magnitude with those in UVA. However, increased differences (up to ~6 and ~3% at the cloud base and the ground respectively) are revealed for higher solar zenith angles. The greatest percentage differences are revealed in SW irradiance. At the cirrus cloud base, the maximum decrease is ~1.5% for the lower solar zenith angles. At 60° and 80° the maximum differences reach 3% and 7.3% respectively.

The disproportionate role of cirrus clouds on the extinction of solar irradiance in the selected spectral bands, due to the different contribution of the direct and the diffuse irradiance components, is presented in Figs. 3 and 4 for two solar zenith angles (80° and 40° respectively). In Fig. 3, the percentage decreases of SW and UVB irradiance at different height levels (0–12 km), due to the cirrus cloudiness (relative to cloud-free irradiance), are presented. The decrease at the cloud base (9 km), due to cloudiness, is more pronounced in SW irradiance. Although it becomes considerably less at the ground, at least two thirds of the estimated decrease at the cloud base is still evident at 2 km. In contrast, the estimated difference in UVB at the cloud base is decreased in the next 3–4 km below the cloud layer and, then, remains almost stable between the 5 km and ground level. The calculated differences due to cloudiness for PAR and UVB are presented in Fig. 4 for a moderate solar zenith angle (40°). In this case, the calculated decrease in PAR at the cloud base is slightly increased at all heights down to the ground levels.

Table 2
Minimum and maximum decreases of UVB, UVA, SW irradiance and PAR at the cloud base and the ground, derived from model calculations over all selected regions due to cirrus cloudiness. Results are presented for four solar zenith angles (SZA) and two months (January, upper panel, and July, lower panel).

	UVB		UVA		PAR		SW	
SZA (°)	Cloud base	Ground	Cloud base	Ground	Cloud base	Ground	Cloud base	Ground
January								
20	–	–	–	–	–	–	–	–
40	0.5–1.2	0.7–1.6	0.5–1.0	0.6–1.5	0.6–1.4	0.5–1.6	0.5–1.6	0.8–1.7
60	0.8–1.8	0.7–1.6	0.9–2.1	0.8–1.8	1.1–2.6	1.1–2.4	1.1–2.8	1.2–2.6
80	0.8–2.2	0.7–1.6	1.4–3.8	0.8–1.8	2.3–5.8	1.3–2.9	2.2–6.4	1.6–3.7
July								
20	0.1–0.5	0.4–1.5	0.2–1.1	0.4–1.5	0.2–0.8	0.3–1.2	0.2–1.1	0.3–1.3
40	0.3–1.1	0.4–1.6	0.3–1.1	0.4–1.5	0.3–1.4	0.4–1.6	0.4–1.6	0.4–1.7
60	0.8–1.9	0.7–1.6	0.5–2.2	0.5–1.9	0.6–2.8	0.6–2.6	0.7–3.0	0.7–2.8
80	0.6–2.4	0.4–1.6	1.3–4.5	0.4–1.9	1.7–6.6	0.8–3.4	1.8–7.3	1.0–4.0

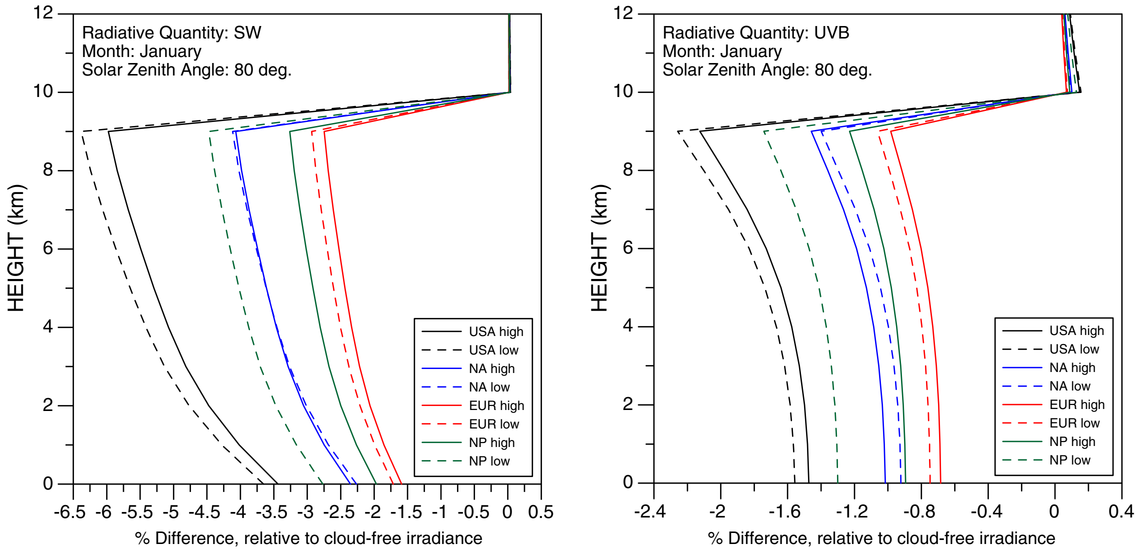

Fig. 3. The percentage (%) decrease of SW (left panel) and UVB (right panel) irradiance over the selected regions during January for a solar zenith angle of 80°, at different height levels, as derived from the model calculations. The cloud layer was placed between 9 and 10 km.

However, due to the enhanced scattering of UVB irradiance, the effect of the cirrus cloud layer is more evident at the ground.

These results correspond to the average effect of cirrus cloudiness over the selected regions on solar irradiance in the four spectral bands. A significantly increased effect is expected over regions with enhanced cirrus cloudiness or during days where the cloud coverage is higher than its mean value. Even with this average situation, cirrus clouds could substantially affect, if correctly accounted for, the quality of the results derived from ground-based measurements and the estimates from satellite instruments and model calculations. In most of the examined cases of this study, the effect of cirrus in solar irradiance is detectable, since it is close to the measurement uncertainties of quality controlled spectroradiometers (e.g. Bais et al., 2001; Grobner et al., 2005; Garane et al., 2006), narrowband radiometers (e.g. Dubovik and King, 2000; Hoiskar et al., 2003; Hülsen et al., 2008; Johnsen et al., 2008) and broadband instruments (e.g. Fairall et al., 1998). If cirrus cloudiness is neither detected nor introduced correctly in processing algorithms of these measurements, it could add significantly on the measurement uncertainties of several atmospheric constituents and especially aerosol optical properties (e.g. Smirnov et al., 2000; Carlund et al., 2003; Kazadzis et al., 2010). The scattering of

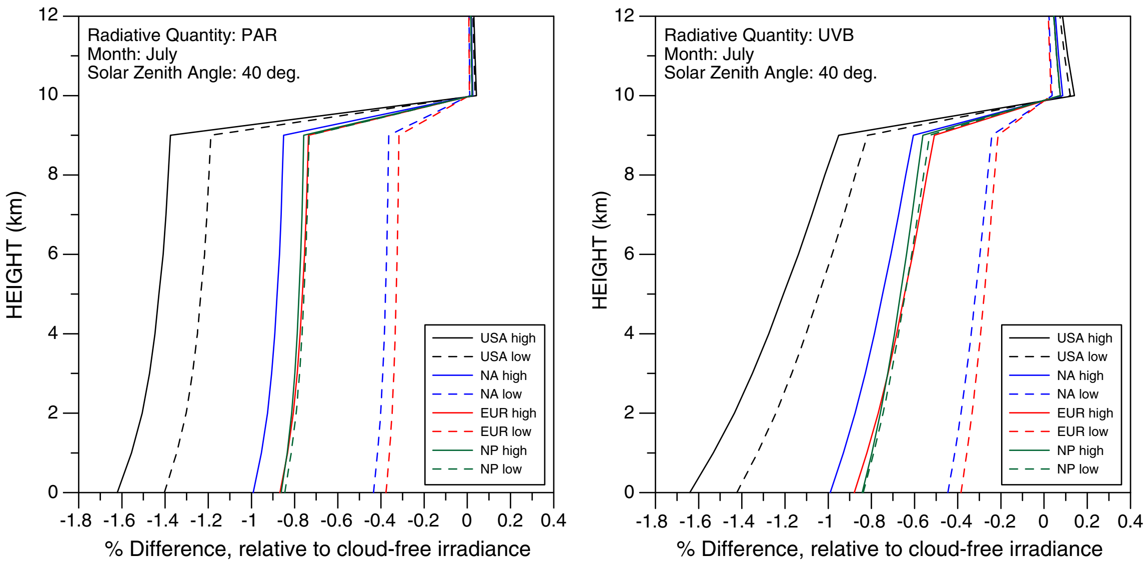

Fig. 4. The percentage (%) decrease of PAR (left panel) and UVB (right panel) irradiance over the selected regions during July for a solar zenith angle of 40°, at different height levels, as derived from the model calculations. The cloud layer was placed between 9 and 10 km.

solar radiation by cirrus clouds often contaminates aerosol products retrieved from remote sensing instruments using channels located in the visible and near-IR spectral region and leads to the overestimation of aerosol optical depth and the underestimation of the Angstrom exponent (Gao et al., 2002).

Similar implications are expected in remote sensing from space of the total amount and vertical profile of tropospheric pollutants (Fishman et al., 2008). In many instances, the cloud masks fail for cases of thin cirrus, due to the fact that passive sensors find it difficult to distinguish in the visible or infrared wavelength range the relatively small signal of thin cirrus from background surface effects. Cloud edges cause further difficulty, since the instrument field of view is not always completely cloudy or clear (Dessler and Yang, 2003; Ackerman et al., 2008; Holz et al., 2007; Lee et al., 2009; Meyer and Platnick, 2010).

Since cirrus clouds cover about 30% of the globe (e.g. Wylie and Menzel, 1999; Stubenrauch et al., 2006), they play an important role in the climate system. Thin cirrus clouds usually cause a positive radiative forcing at the top of the atmosphere, while thick cirrus clouds may produce cooling (Stephens and Webster, 1981; Fu and Liou, 1993; Fahey and Schumann, 1999; Boudala et al., 2007). Due to the significant uncertainties regarding their radiative and climate effect (Intergovernmental Panel on Climate Change, in Climate Change, 2007), the evaluation of cirrus parameterizations for the computation of radiative flux computations in climate models is a field of on-going research (Stubenrauch et al., 2007; Myhre et al., 2009; Hendricks et al., 2010; Wang and Penner, 2010).

The above-mentioned differences in model derived irradiance due to cirrus cloudiness indicate that, when cirrus clouds are present, their distribution and optical properties must be well known for accurate model calculations or high-quality airborne measurements in the troposphere, especially for high solar zenith angles.

5. Conclusions

In the present study, we used cirrus cloud data (optical depth and coverage) from the ISCCP during the 1984–2007 time period as model inputs in a spectral radiative transfer algorithm. Our aim was to estimate, for the first time, the impact of cirrus clouds on selected solar irradiance integrals (UVB, UVA, PAR and SW) at different heights in the troposphere.

The magnitude of the calculated differences depends on the selected solar zenith angle and is generally minimum in UVB and maximum in SW. Although the results refer to average cirrus cloud conditions, they are, in many cases, comparable with the typical measurement uncertainties of ground-based or satellite instruments. According to the instrument accuracy and the processing algorithms used, the development of suitable detection methods and parameterizations of cirrus optical properties is recommended, in order to reduce the uncertainties in calculations of atmospheric constituents (especially aerosols) in the troposphere. The development of new observational capabilities (from ground and space) has already led to new insights into atmospheric processes and the focus on the determination of cirrus cloud properties should be a near-term priority. In this way, both the improved accuracy in tropospheric measurements and the adequate evaluation of cirrus impact on climate would be fulfilled.

Acknowledgments

This study was mainly conducted within the FP6 Integrated Project QUANTIFY (003893-GOCE), funded by EU.

It was also partly supported by project “Hellenic Network of Solar Energy” (HNSE), funded by the General Secretariat for Research and Technology, Greek Ministry of Education, Lifelong Learning and Religious Affairs.

The LibRadtran team (www.libradtran.org) is acknowledged for providing the model algorithm.

The ISCCP D2 data were obtained from the International Satellite Cloud Climatology Project web site http://isccp.giss.nasa.gov maintained by the ISCCP research group at the NASA Goddard Institute for Space Studies, New York, NY.

References

Ackerman, S.A., Holz, R.E., Frey, R., Eloranta, E.W., Maddux, B.C., McGill, M., 2008. Cloud detection with MODIS. Part II: validation. J. Atmos. Oceanic Technol. 25, 1073–1086.

Anderson, G.P., Clough, S.A., Kneizys, F.X., Chetwynd, J.H., Shettle, E.P., 1986. AFGL Atmospheric Constituent Profiles (0–120 km). AFGL-TR-86-0110, AFGL (OPI), Hanscom AFB, MA 01736. .

Bais, A.F., Gardiner, B.G., Slaper, H., Bluthaler, M., Bernhard, G., McKenzie, R., Webb, A.R., Seckmeyer, G., Kjeldstad, B., Koskela, T., Kirsch, P.J., Gröbner, J., Kerr, J.B., Kazadzis, S., Leszczynski, K., Wardle, D., Josefsson, W., Brognies, C., Gillotay, D., Reinen, H., Weihs, P., Svenoe, T., Eriksen, P., Kuik, F., Redondas, A., 2001. A SUSPEN intercomparison of ultraviolet spectroradiometers. J. Geophys. Res. 106 (D12), 12509–12525.

Bais, A.F., Kazantzidis, A., Kazadzis, S., Balis, D.S., Zerefos, C.S., Meleti, C., 2005. Deriving an effective aerosol single scattering albedo from spectral surface UV irradiance measurements. Atmos. Environ. 39, 1093–1102.

Bernhard, G., Seckmeyer, G., McKenzie, R.K., Johnston, P.V., 1998. Ratio spectra as a quality control tool for solar spectral measurements. J. Geophys. Res. 103 (D22), 28855–28861.

Bernhard, G., Booth, C.R., Ehramjian, J.C., Nichol, S.E., 2006. UV climatology at McMurdo Station, Antarctica, based on version 2 data of the National Science Foundation's ultraviolet monitoring network. J. Geophys. Res. 111. doi:10.1029/2005JD005857.

Blumthaler, M., Schallhart, B., Schwarzmann, M., McKenzie, R., Johnston, P., Kotkamp, M., Shiona, H., 2008. Spectral UV measurements of global irradiance, solar radiance, and actinic flux in New Zealand: intercomparison between instruments and model calculations. J. Atmos. Oceanic Technol. 25 (6), 945–958.

Borde, R., Verdebout, J., 2003. Remote sensing of aerosols optical thickness over various sites using SeaWIFS or VEGETATION and ground measurements. Remote Sens. Environ. 86, 42–51.

Boudala, F.S., Isaac, G.A., McFarlane, N.A., Li, J., 2007. The sensitivity of the radiation budget in a climate simulation to neglecting the effect of small ice particles. J. Climate 20, 3527–3541.

Burkhardt, U., Kärcher, B., Schumann, U., 2010. Global modeling of the contrail and contrail cirrus climate impact. Bull. Am. Meteorol. Soc. 91, 479–483.

Cahalan, R.F., Oreopoulos, L., Marshak, A., Evans, K.F., Davis, A., Pincus, R., Yetzer, K., Mayer, B., Davies, R., Ackerman, T.P., Barker, H.W., Clothiaux, E.E., Ellingson, R.G., Garay, M.J., Kassianov, E., Kinne, S., Macke, A., O'Hirok, W., Partain, P.T., Prigarin, S.M., Rublev, A.N., Stephens, G.L., Szczap, F., Takara, E.E., Varnai, T., Wen, G., Zhuraleva, T.B., 2005. The International Intercomparison of 3D Radiation Codes (I3RC): bringing together the most advanced radiative transfer tools for cloudy atmospheres. Bull. Am. Meteorol. Soc. 86 (9), 1275–1293.

Carlund, T., Landelius, T., Josefsson, W., 2003. Comparison and uncertainty of aerosol optical depth estimates derived from spectral and broadband measurements. J. Appl. Meteor. 42, 1598–1610.

Cerdena, A., Gonzalez, A., Perez, J.C., 2007. Remote sensing of water cloud parameters using neural networks. J. Atmos. Oceanic Technol. 24, 52–63.

Dessler, A.E., Yang, P., 2003. The distribution of tropical thin cirrus clouds inferred from Terra MODIS data. J. Clim. 16, 1241–1247.

Dubovik, O., King, M.D., 2000. A flexible inversion algorithm for retrieval of aerosol optical properties from Sun and sky radiance measurements. J. Geophys. Res. 105, 20673–20696.

Edwards, J.M., Havemann, S., Thelen, J.-C., Baran, A.J., 2007. A new parameterization for the radiative properties of ice crystals: comparison of existing schemes and impact in a GCM. Atmos. Res. 83 (1), 19–35.

Ehrlich, A., Wendisch, M., Bierwirth, E., Gayet, J.-F., Mioche, G., Lampert, A., Mayer, B., 2009. Evidence of ice crystals at cloud top of Arctic boundary-layer mixed-phase clouds derived from airborne remote sensing. Atmos. Chem. Phys. 9, 9401–9416.

Eleftheratos, K., Zerefos, C.S., Zanis, P., Balis, D.S., Tselioudis, G., Gierens, K., Sausen, R., 2007. A study on natural and manmade global interannual fluctuations of cirrus cloud cover for the period 1984–2004. Atmos. Chem. Phys. 7, 2631–2642.

Fahey, D.W., Schumann, U., 1999. Aviation-produced aerosols and cloudiness, Chapters 3 in aviation and global atmosphere. In: Penner, J.E., Griggs, D.H., Dokken, D.J., McFarland, M. (Eds.), A Special Report of IPCC (Intergovernmental Panel on Climate Change). Cambridge University Press, Cambridge, UK, pp. 65–120.

Fairall, C.W., Persson, P.O.G., Bradley, E.F., Payne, R.E., Anderson, S.P., 1998. A new look at calibration and use of Eppley precision infrared radiometers. Part I: theory and application. J. Atmos. Oceanic Technol. 15, 1229–1242.

Fishman, J., Bowman, K.W., Burrows, J.P., Richter, A., Chance, K.V., Edwards, D.P., Martin, R.V., Morris, G.A., Pierce, R.B., Ziemke, J.R., Al-Saadi, J.A., Creilson, J.K., Schaack, T.K., Thompson, A.M., 2008. Remote sensing of tropospheric pollution from space. Bull. Am. Meteorol. Soc. 89, 805–821.

Fu, Q., 1996. An accurate parameterization of the solar radiative properties of cirrus clouds in climate models. J. Climate 9, 2058–2082.

Fu, Q., Liou, K.N., 1993. Parameterization of the radiative properties of cirrus clouds. J. Atmos. Sci. 50, 2008–2025.

Gao, B.C., Kaufman, Y.J., Tanre, D., Li, R.R., 2002. Distinguishing tropospheric aerosols from thin cirrus clouds for improved aerosol retrievals using the ratio of 1.38-μm and 1.24-μm channels. Geophys. Res. Lett. 29. doi:10.1029/2002GL015475 No. 18, 1890.

Garane, K., Bais, A.F., Kazadzis, S., Kazantzidis, A., Meleti, C., 2006. Monitoring of UV spectral irradiance at Thessaloniki (1990–2005): data re-evaluation and quality control. Ann. Geophysicae 24, 1–14.

Grobner, J., Schreder, J., Kazadzis, S., Bais, A.F., Blumthaler, M., Gorts, P., Tax, R., Koskela, T., Seckmeyer, G., Webb, A.R., Rembges, D., 2005. Traveling reference spectroradiometer for routine quality assurance of spectral solar ultraviolet irradiance measurements. Appl. Opt. 44 (25), 5321–5331.

Hendricks, J., Falb, A., Stubenrauch, C.J., Emde, C., 2010. A method for comparing properties of cirrus clouds in global climate models with those retrieved from IR sounder satellite observations. Meteorol. Z. 19 No. 6, 577–589.

Hoiskar, B.A.K., Haugen, R., Danielsen, T., Kylling, A., Edvardsen, K., Dahlback, A., Johnsen, B., Blumthaler, M., Schreder, J., 2003. Multichannel moderate-bandwidth filter instrument for measurement of the ozone-column amount, cloud transmittance, and ultraviolet dose rates. Appl. Opt. 42 (18), 3472–3479.

Holz, R.E., Ackerman, S.A., Nagle, F.W., Frey, R., Dutcher, S., Kuehn, R.E., Vaughan, M.A., Baum, B., 2007. Global Moderate Resolution Imaging Spectroradiometer (MODIS) cloud detection and height evaluation using CALIOP. J. Geophys. Res. 113. doi:10.1029/2008JD009837 D00A19.

Hülsen, G., Gröbner, J., Bais, A., Blumthaler, M., Disterhoft, P., Johnsen, B., Lantz, K.O., Meleti, C., Schreder, J., Guerrero, J.M.V., Ylianttila, L., 2008. Intercomparison of erythemal broadband radiometers calibrated by seven UV calibration facilities in Europe and the USA. Atmos. Chem. Phys. 8 (16), 4865–4875.

Intergovernmental Panel on Climate Change, in Climate Change, 2007. The Physical Science Basis. Contribution of Working Group I to the Fourth Assessment Report of the Intergovernmental Panel on Climate Change. Cambridge University Press, Cambridge, United Kingdom and New York, NY, USA.

Jin, Y., Rossow, W.B., Wylie, D.P., 1996. Comparison of the climatologies of high level clouds from HIRS and ISCCP. J. Climate 9, 2850–2879.

Johnsen, B., Kjeldstad, B., Aalerud, T.N., Nilsen, L.T., Schreder, J., Blumthaler, M., Bernhard, G., Topaloglou, C., Meinander, O., Bagheri, A., Slusser, J.R., Davis, J., 2008. Intercomparison and harmonization of UV Index measurements from multiband filter radiometers. J. Geophys. Res. 113 (D15), D15206.

Kazadzis, S., Gröbner, J., Arola, A., Amiridis, V., 2010. The effect of the global UV irradiance measurement accuracy on the single scattering albedo retrieval. Atmos. Meas. Tech. 3 (4), 1029–1037.

Kazantzidis, A., Balis, D.S., Bais, A.F., Kazadzis, S., Galani, E., Kosmidis, E., Blumthaler, M., 2001. Comparison of model calculations with spectral UV measurements during the SUSPEN campaign: the effect of aerosols. J. Atmos. Sci. 1529–1539.

Kinne, S., Schulz, M., Textor, C., Guibert, S., Balkanski, Y., Bauer, S.E., Berntsen, T., Berglen, T.F., Boucher, O., Chin, M., Collins, W., Dentener, F., Diehl, T., Easter, R., Feichter, J., Fillmore, D., Ghan, S., Ginoux, P., Gong, S., Grini, A., Hendricks, J.E., Herzog, M., Horowitz, L., Isaksen, I., Iversen, T., Kirkavag, A., Kloster, S., Koch, D., Kristjansson, J.E., Krol, M., Lauer, A., Lamarque, J.F., Lesins, G., Liu, X., Lohmann, U., Montanaro, V., Myhre, G., Penner, J.E., Pitari, G., Reddy, S., Seland, O., Stier, P., Takemura, T., Tie, X., 2006. An AeroCom initial assessment — optical properties in aerosol component modules of global models. Atmos. Chem. Phys. 6, 1815–1834.

Kokhanovsky, A., Mayer, B., von Hoyningen-Huene, W., 2007. Retrieval of cloud spherical albedo from top-of-atmosphere reflectance measurements performed at a single observation angle. Atmos. Chem. Phys. 7, 3633–3637.

Kurucz, R.L., 1992. In: Rabin, D.M., Jefferies, J.T. (Eds.), Synthetic Infrared Spectra in Infrared Solar Physics, IAU Symp. 154. Kluwer, Acad, Norwell, MA.

Kylling, A., Bais, A.F., Blumthaler, M., Schreder, J., Zerefos, C.S., Kosmidis, E., 1998. Effect of aerosols on solar UV irradiances during the photochemical activity and solar ultraviolet radiation campaign. J. Geophys. Res. 103 (20), 26051–26060.

Lee, J., Yang, P., Dessler, A.E., Gao, B.-C., Platnick, S., 2009. Distribution and radiative forcing of tropical thin cirrus clouds. J. Atmos. Sci. 66 (12), 3721–3731.

Liao, X., Rossow, W.B., Rind, D., 1995. Comparison between SAGE II and ISCCP high level clouds, Part I: global and zonal mean cloud amounts. J. Geophys. Res. 100, 1121–1135.

Liou, K.N., 1986. Influence of cirrus clouds on weather and climate processes: a global prespective. Mon. Weather Rev. 114, 1167–1199.

Liou, K.N., 2005. Cirrus Clouds and Climate. In McGraw&Hill 2005 Yearbook of Science and Technology. McGraw&Hill, New York, pp. 51–53.

Loyola, D.G., Thomas, W., Spurr, R., Mayer, B., 2010. Global patterns in daytime cloud properties derived from GOME backscatter UV–VIS measurements. Int. J. Remote Sens. 31 (16), 4295–4318.

Lynch, D.K., 1996. Cirrus clouds: their role in climate and global change. Acta Astronaut. 38, 859–863.

Mayer, B., Kylling, A., 2005. Technical note: the libRadtran software package for radiative transfer calculations — description and examples of use. Atmos. Chem. Phys. 5, 1855–1877.

Meerkötter, R., Bugliaro, L., 2009. Diurnal evolution of cloud base heights in convective cloud fields from MSG/SEVIRI data. Atmos. Chem. Phys. 9, 1767–1778.

Meerkötter, R., Schumann, U., Doelling, D.R., Minnis, P., Nakajima, T., Tsushima, Y., 1999. Radiative forcing by contrails. Ann. Geophys. 17, 1080–1094. doi:10.1007/s00585-999-1080-7.

Meloni, D., Di Sarra, A., Pace, G., Monteleone, F., 2006. Aerosol optical properties at Lampedusa (Central Mediterranean). 2. Determination of single scattering albedo at two wavelengths for different aerosol types. Atmos. Chem. Phys. 6, 715–727.

Meyer, K., Platnick, S., 2010. Utilizing the MODIS 1.38 mm channel for cirrus cloud optical thickness retrievals: algorithm and retrieval uncertainties. J. Geophys. Res. 115, D24209. doi:10.1029/2010JD014872.

Min, M., Wang, P., Campbell, J.R., Zong, X., Li, Y., 2010. Midlatitude cirrus cloud radiative forcing over China. J. Geophys. Res. 115, D20210. doi:10.1029/2010JD014161.

Myhre, G., Kvalevåg, M., Rädel, G., Cook, J., Shine, K.P., Clark, H., Karcher, F., Marcowicz, K., Kardas, A., Wolkenberg, P., Balkanski, Y., Ponater, M., Forster, P., Rap, A., de Leon, R.R., 2009. Intercomparison of radiative forcing calculations of stratospheric water clouds and contrails. Meteorol. Z. 18 (6), 585–596.

O'Hirok, W., Gautier, C., 2003. Absorption of shortwave radiation in a cloudy atmosphere: observed and theoretical estimates during the second Atmospheric Radiation Measurement Enhanced Shortwave Experiment (ARESE). J. Geophys. Res. 108, 4412. doi:10.1029/2002JD002818.

Pilewskie, P., Pommier, J., Bergstrom, R., Gore, W., Howard, S., Rabbette, M., Schmid, B., Hobbs, P.V., Tsay, S.C., 2003. Solar spectral radiative forcing during the Southern African Regional Science Initiative. J. Geophys. Res. 108 (D13), 8486.

Ramanathan, V., Cess, R.D., Harrison, E.F., Minnis, P., Barkstrom, B.R., Ahmad, E., Hartmann, D., 1989. Cloud radiative forcing and climate: results from the Earth Radiation Budget Experiment. Science 243, 57–63. doi:10.1126/science.243.4887.57.

Rossow, W.B., Schiffer, R.A., 1991. ISCCP cloud data products. Bull. Amer. Meteor. Soc. 72, 2–20.

Rossow, W.B., Schiffer, R.A., 1999. Advances in understanding clouds from ISCCP. Bull. Amer. Meteor. Soc. 80, 2261–2287.

Schmidt, K.S., Venema, V., Di Giuseppe, F., Scheirer, R., Wendisch, M., Pilewskie, P., 2007. Reproducing cloud microphysical and irradiance measurements using three 3D cloud generators. Q. J. R. Meteorol. Soc. 133, 765–780. doi:10.1002/qj.53.

Schmidt, K.S., Pilewskie, P., Mayer, B., Wendisch, M., Kindel, B., Platnick, S., King, M.D., Wind, G., Tom Arnold, G., Tian, L., Heymsfield, G., Kalesse, H., 2010. Apparent absorption of solar spectral irradiance in heterogeneous ice clouds. J. Geophys. Res. 115, D00J22. doi:10.1029/2009JD013124.

Schumann, U., 2010. A contrail cirrus prediction tool. In: Sausen, R., van Velthoven, P.F.J., Brüning, C., Blum, A. (Eds.), Proceedings of the 2nd International Conference on Transport, Atmosphere and Climate: June 22nd to 25th 2009, Aachen and Maastricht, pp. 69–74.

Schumann, U., Mayer, B., Graf, K., Mannstein, H., Meerkotter, R., 2009. A parametric radiative forcing model for cirrus and contrail cirrus. ESA Atmospheric Science Conference: Special Publication SP-676 (6 pages), Barcelona, Spain, 7–11 September 2009.

Shettle, E.P., 1989. Models of aerosols, clouds and precipitation for atmospheric propagation studies. In AGARD Conference Proceedings No. 454, Atmospheric propagation in the uv, visible, ir and mm-region and related system aspects.

Smirnov, A., Holben, B.N., Eck, T.F., Dubovik, O., Slutsker, I., 2000. Cloud screening and quality control algorithms for the AERONET database. Rem. Sens. Env. 73, 337–349.

Stephens, G.L., Webster, P.J., 1981. Clouds and climate: sensitivity of simple systems. J. Atmos. Sci. 38, 235–247.

Stordal, F., Myhre, G., Stordal, E.J.G., Rossow, W.B., Lee, D.S., Arlander, D.W., Svendby, T., 2005. Is there a trend in cirrus cloud cover due to air traffic? Atmos. Chem. Phys. 5, 2155–2162.

Stubenrauch, C.J., Rossow, W.B., Cheruy, F., Chedin, A., Scott, N.A., 1999. Clouds as seen by satellite sounders (3I) and imagers (ISCCP). Part 1: evaluation of cloud parameters. J. Climate 12, 2189–2213.

Stubenrauch, C.J., Chédin, A., Rädel, G., Scott, N.A., Serrar, S., 2006. Cloud properties and their seasonal and diurnal variability from TOVS Path-B. J. Climate 19, 5531–5553.

Stubenrauch, C.J., Eddounia, F., Edwards, J.M., Macke, A., 2007. Evaluation of cirrus parameterizations for radiative flux computations in climate models using TOVS-ScaRaB satellite observations. J. Climate 20, 4459–4475.

Van Weele, M., Martin, T.J., Blumthaler, M., Brogniez, C., den Outer, P.N., Engelsen, O., Lenoble, J., Pfister, G., Ruggaber, A., Walravens, B., Weihs, P., Dieter, H., Gardiner, B.G., Gillotay, D., Kylling, A., Mayer, B., Seckmeyer, G., Wauben, W., 2000. From model intercomparisons towards benchmark UV spectra for six real atmospheric cases. J. Geophys. Res. 105 (D4), 4915–4925.

Wang, M., Penner, J.E., 2010. Cirrus clouds in a global climate model with a statistical cirrus cloud scheme. Atmos. Chem. Phys. 10, 5449–5474.

Webb, A.R., Kylling, A., Wendisch, M., Jäkel, E., 2004. Airborne measurements of ground and cloud spectral albedos under low aerosol loads. J. Geophys. Res. 109. doi:10.1029/2004JD004768.

Wendisch, M., Müller, D., Schell, D., Heintzenberg, J., 2001. An airborne spectral albedometer with active horizontal stabilization. J. Atmos. Oceanic Technol. 18, 1856–1866.

Wendisch, M., Pilewski, P., Jäkel, E., Schmidt, S., Pommier, J., Howard, S., Jonsson, H.H., Guan, H., Schröder, M., Mayer, B., 2004. Airborne measurements of areal spectral surface albedo over different sea and land surfaces. J. Geophys. Res. 109 (D8). doi:10.1029/2003JD004392.

Wylie, D.P., Menzel, W.P., 1999. Eight years of cloud statistics using HIRS. J. Climate 12, 170–184.

Yang, P., Hong, G., Dessler, A., Ou, S., Liou, K., Minnis, P., Harshvardhan, 2010. Contrails and induced cirrus: optics and radiation. Bull. Amer. Meteor. Soc. 91, 473–478.

Zerefos, C.S., Eleftheratos, K., Balis, D.S., Zanis, P., Tselioudis, G., Meleti, C., 2003. Evidence of impact of aviation on cirrus cloud formation. Atmos. Chem. Phys. 3, 1633–1644.

Zerefos, C.S., Eleftheratos, K., Zanis, P., Balis, D.S., Tselioudis, G., 2007. Search for man-made cirrus contrails over Southeast Asia. Terrestrial Atmos. Oceanic Sci. 18 (3), 459–474. doi:10.3319/TAO.2007.18.3.459(EA).